A combined tracking and registration approach for tracking anatomical landmarks in 4D ultrasound of the liver

Jyotirmoy Banerjee[1,2], Camiel Klink[1], Erwin Vast[1,2], Wiro J. Niessen[1,2], Adriaan Moelker[1] and Theo van Walsum[1,2]

[1] Dept. of Radiology, Erasmus MC, Rotterdam, The Netherlands
[2] Dept. of Medical Informatics, Erasmus MC, Rotterdam, The Netherlands
{*j.banerjee, t.vanwalsum*}*@erasmusmc.nl*

Abstract. In this paper we present a method for tracking of anatomical landmarks in the liver. Our 4D ultrasound tracking method is based on global and local rigid registration schemes. We evaluate our method on the dataset that was presented in the MICCAI 2015 Challenge on Liver Ultrasound Tracking (CLUST 2015). On the test set a mean tracking error of 1.62 ± 0.94 mm is achieved.

1 Introduction

Ultrasound (US) is used by clinicians to image the human anatomy. It is an inexpensive, non-invasive and portable imaging modality. It is widely used in diagnostics. As US imaging is real-time it can be used for interventions and therapy. The anatomy can be tracked real-time. Some of the applications are tissue motion analysis and image guidance during interventions. One of the main purpose of an US tracking approach is to incorporate (pre-operative) planning information (to guide visualization), or to integrate preoperative imaging data during interventions. Tracking or motion compensation algorithms helps to negate the motion caused by the probe or the patient and the breathing motion in particular.

Several methods for tracking of anatomical landmarks [5, 7, 8] and motion tracking of liver [4, 6, 9–12] in US have been proposed in literature. Our method is based on the previous work described in Banerjee et al. [2] and [3]. The previous methods were developed to track/register US liver volumes. In this work these methods are used to perform the specific task of tracking anatomical landmarks in the liver. The method is evaluated on the CLUST 2015 challenge datasets.

2 Tracking anatomical landmarks

We briefly review the register to reference strategy (RTR) [3] in Subsection 2.1 and the register to reference by tracking strategy (RTRT) [2] in Subsection 2.2 which are the core components of our landmark tracking approach. In Subsection 2.3 we discuss the landmark tracking approach, see the block diagram in Figure 1.

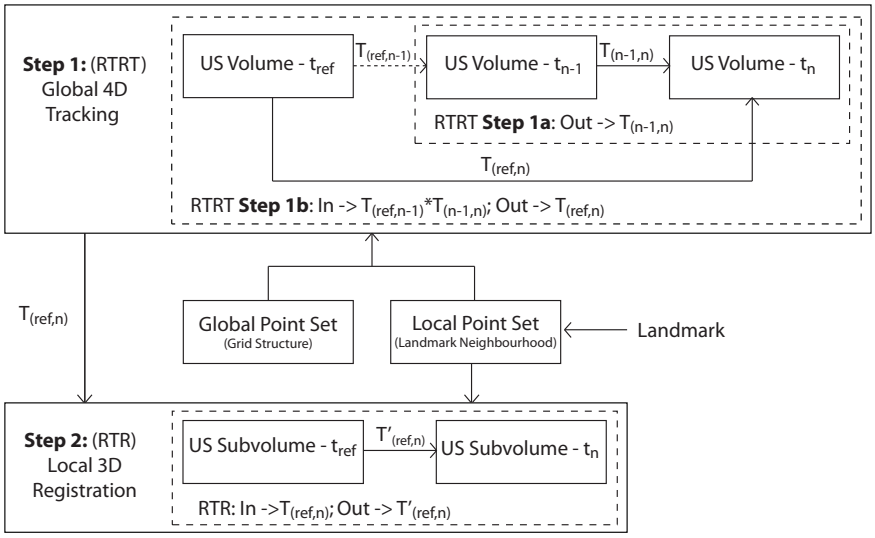

Fig. 1. Block diagram - tracking of anatomical landmarks.

2.1 Step 1: RTR [3]

The RTR approach [3] is a 3D to 3D US registration technique where the streaming input frame (t_n) is directly registered to the reference frame (t_{ref}). It is based on a block-matching scheme followed by an outlier-rejection scheme. For a set of points (generated using a grid structure or a Gaussian distribution, see the global point set and the local point set in Figure 2) located in the fixed image, block-matching is used to find corresponding locations in the moving image. The correspondences from the block-matching are inputs to the outlier rejection scheme. The outlier rejection scheme uses geometric and appearance consistency criteria to determine the block-matching results that can be trusted. The method then uses only the selected block-matching results from the outlier rejection scheme to estimate a rigid transformation using the approach described by Arun et al. [1]. For details refer [3].

2.2 Step 2: RTRT [2]

The RTRT approach [2] is a 4D US registration/tracking technique, where the registration is performed in two steps. In the first step (Step 1a), the streaming input frame (t_n) is registered to the previous frame in the temporal domain (t_{n-1}). In the second step (Step 1b), the previously estimated transformation ($T_{(ref,n-1)}$) and the transformation from the first step ($T_{(n-1,n)}$) are used to initialize the registration between the streaming input frame and the reference frame, by composing the transformations as $T_{(ref,n-1)} * T_{(n-1,n)}$. To reduce the accumulation of error the reference frame is re-registered to the streaming input frame which was earlier transformed using the transformation $T_{(ref,n-1)} * T_{(n-1,n)}$, resulting in the final transformation, written as $T_{(ref,n)}$, see

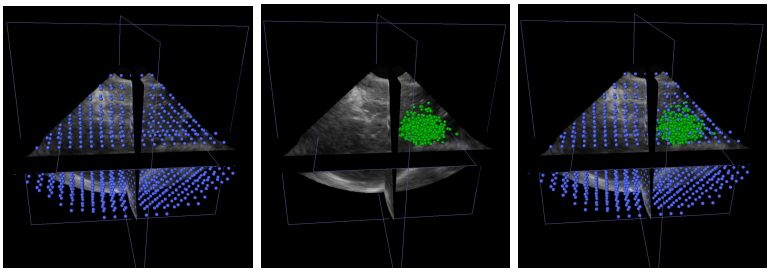

Fig. 2. Global and local point set: Left - Global point set generated using a grid structure (blue color), Middle - Local point set (green color), Right - Global cum local point set generated using a Gaussian distribution (σ=10 mm).

Figure 1. The RTRT approach additionally performs efficient tracking of points in the temporal domain. The tracking starts with a set of ℓ points (generated using a grid structure or a Gaussian distribution, see the global point set and the local point set in Figure 2) located in the fixed/reference image. Points that are consistently tracked are retained and the rest of the points are rejected. Additional points are introduced from a distribution (could be the same distribution as used earlier) if the number of points for tracking is less than ℓ. For details refer [2]. Note that in the next cycle of the RTRT approach, the current estimated transformation $T_{(ref,n)}$ is used in determining the transformation between the reference volume (t_{ref}) and the next US volume (t_{n+1}), written as $T_{(ref,n+1)}$.

2.3 Tracking landmarks

The anatomical landmark tracking approach, see Figure 1, consists of the following two rigid registration steps. First, in the *global* 4D registration/tracking step, the RTRT strategy is used track the whole (liver) US volume ($T_{(ref,n)}$). Second, in the *local* 3D registration step, we refine the tracking result by performing registration using the neighborhood region close to the anatomical landmark ($T'_{(ref,n)}$).

Both the RTR and RTRT strategies use block-matching followed by an outlier rejection scheme to find correspondences between the US volumes. Input to the block-matching module is a point set. The portion/region of the image used for the registration/tracking is determined by the locations of the points in the US volume. As shown in the block diagram in Figure 1, a combination of a global and a local point set is used to perform a global 4D tracking/registration and only a local point set is used to perform a local 3D registration. The global point set is generated using a grid structure spread over the entire US volume, the local point set is a collection of points in the neighborhood of the anatomical landmark (see Figure 2).

3 Experiment and results

The CLUST 2015 challenge dataset is used to evaluate the performance of the method. The challenge contained 16 4D sequences from multiple sources. The

Table 1. Summary of the data

Source	Traning Sequences	Test Sequences	Image size [voxels]	Image res. [mm]	Frame rate [Hz]	Scanner	Probe
EMC	3	2	192x246x117	1.14x0.59x1.19	6	Philips iU22	X6-1
ICR	1	1	480x120x120	0.31x0.51x0.67	24	Siemens SC2000	4Z1c
SMT	4	5	227x227x229	0.70x0.70x0.70	8	GE E9	4V-D

summary of the data is shown in Table 1. The data was divided into a training set of 8 4D sequences and a test set of 8 4D sequences. For tuning the algorithm, annotations (i.e. landmarks) across multiple frames per 4D sequence were provided for the training set. For the test set, one or more annotations in the first frame were provided. These annotated landmarks were tracked over time. The tracking performance of the test set was evaluated by the organizers of the challenge. The Euclidean distance between the tracked points and manual annotations was calculated. The error was summarized by the following statistics: mean, standard deviation, 95 percentile, minimum and maximum distances.

MeVisLab, OpenCL and C++ are used for software development. The OpenCL code was run on a NVIDIA GTX 780 Ti GPU.

Parameter setting : We used a block-size of 11^3 mm^3 for the block-matching. The block is evenly sampled 18x18x18 times. The similarity metric used is normalized cross correlation (NCC), $(\sigma_A, \lambda, \sigma_B) = (0.1, 0.1, 0.1)$ is used as the outlier rejection parameters. These values were optimized in the previous work [3]. The number of points for the block-matching (step one and step two) of the RTRT approach and the RTR approach are set to 100, 200 and 400 points, respectively. The search range for the block-matching (step one and step two) of the RTRT approach and the RTR approach is set to 40^3 mm^3, 10^3 mm^3 and 20^3 mm^3, respectively. The search range (step one and step two) of the RTRT approach and the RTR approach are evenly sampled 60x60x60 times, 15x15x15 times and 30x30x30 times, respectively. The sampling determines the step size for the block-matching. A local point set of 1000 points is generated using a Gaussian distribution with mean located at the anatomical landmark and standard deviation of 10 mm. The adjacent horizontal/vertical nodes of the grid structure used to generate the global point set are 10 mm apart, see Figure 2. The points required for the block-matching in the RTR and the RTRT approaches are sampled from the global and the local point sets.

The training set and the test set results are presented in Table 2 and Table 3, respectively. The mean tracking error for the training set and the test set are 3.26 ± 2.62 mm and 1.62 ± 0.94 mm, respectively. The average run time of the Step 1 (RTRT) and the Step 2 (RTR) of our approach as shown in Figure 1 are 6.68 seconds and 4.18 seconds, respectively. Hence for the given parameter settings the GPU implementation runs at 11 seconds per frame.

Table 2. Training set results

Landmarks	Mean (in mm)	Std (in mm)	95th% (in mm)	Min (in mm)	Max (in mm)
EMC-01_1	0.94	0.51	1.65	0.36	1.79
EMC-02_1	1.19	0.47	1.83	0.80	2.01
EMC-02_2	2.28	1.10	3.62	1.02	3.80
EMC-02_3	2.05	0.58	2.80	1.48	2.96
EMC-02_4	1.80	0.54	2.39	1.14	2.41
EMC-03_1	5.55	2.28	8.20	1.78	8.54
EMC	3.01	2.42	7.85	0.36	8.54
ICR-01_1	1.57	0.56	2.36	0.27	2.83
SMT-01_1	2.06	0.41	2.74	1.08	2.97
SMT-01_2	3.46	0.55	4.43	2.42	4.61
SMT-01_3	3.00	0.42	3.75	1.91	3.89
SMT-02_1	1.65	1.60	2.20	0.6	16.49
SMT-02_2	1.92	0.47	2.74	0.91	3.27
SMT-02_3	3.72	0.70	4.79	2.30	5.59
SMT-03_1	2.29	0.72	3.43	1.19	3.62
SMT-03_2	2.09	0.60	3.14	0.68	3.54
SMT-04_1	8.88	3.82	15.04	0.97	15.31
SMT	3.30	2.64	9.20	0.60	16.49
Tracking Results	3.26	2.62	8.55	0.27	16.49

Table 3. Test set results

Landmarks	Mean (in mm)	Std (in mm)	95th% (in mm)	Min (in mm)	Max (in mm)
EMC-04_1	1.10	0.63	2.28	0.26	2.31
EMC-05_1	1.79	0.36	2.16	1.15	2.17
EMC	1.45	0.61	2.18	0.26	2.31
ICR-02_1	1.65	0.37	2.14	0.80	2.15
SMT-05_1	3.39	2.53	10.13	0.90	10.24
SMT-05_2	0.97	0.36	1.58	0.21	1.91
SMT-06_1	1.56	0.37	2.11	0.57	2.49
SMT-06_2	2.01	0.52	2.77	0.99	3.69
SMT-06_3	1.37	0.35	1.95	0.43	2.18
SMT-07_1	1.83	0.42	2.49	1.02	2.92
SMT-07_2	1.79	0.39	2.46	1.04	2.69
SMT-08_1	1.48	0.41	2.26	0.22	2.44
SMT-08_2	1.09	0.29	1.52	0.37	1.77
SMT-08_3	2.10	0.73	3.37	0.87	3.91
SMT-09_1	1.10	0.35	1.70	0.14	1.89
SMT-09_2	0.96	0.38	1.66	0.10	1.87
SMT-09_3	2.25	0.60	3.16	0.18	3.73
SMT	1.63	0.94	2.86	0.10	10.24
Tracking Results	1.62	0.93	2.84	0.10	10.24

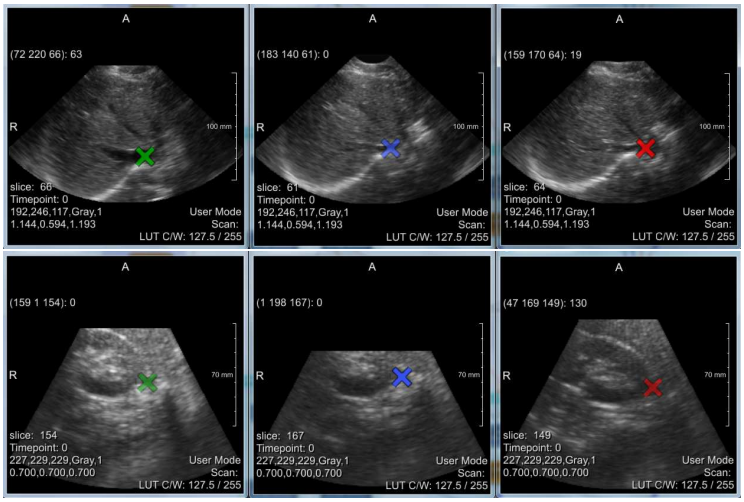

Fig. 3. Training set tracking results: Left - Reference image manual annotation, Middle - Moving image automatic annotation, Right - Moving image manual annotation. Row 1 - For the dataset EMC-03_1 at time point 42, the tracking error is 8.54 mm; Row 2 - For the dataset SMT-04_1 at time point 76, the tracking error is 15.14 mm.

4 Discussion and conclusions

In this paper we perform the task of tracking anatomical landmarks using a combination of previous methods by Banerjee et al. [2] and [3]. A mean tracking error of 1.62 ± 0.94 mm is achieved on the test set. In the first step, the point set used for the global 4D tracking step is a combination of a global point set generated from a grid structure and the local point set generated randomly in the neighborhood of the anatomical landmark. This combination of point set ensures a high percentage of points close to the landmark position during the global 4D tracking step. The local point set is intended to track a specific landmark well, whereas the global point set helps in increasing robustness in tracking. In the second step, the local point set is again used in the local 3D registration step. This step is designed to track the landmark in the presence of local deformations.

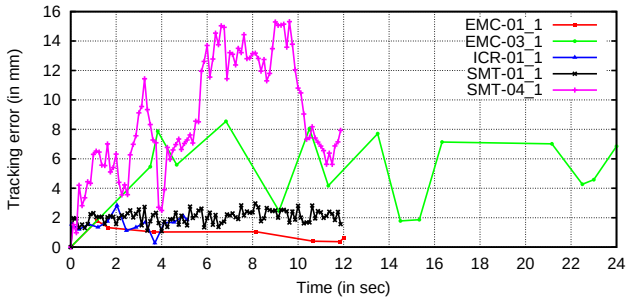

Fig. 4. Tracking examples from the training set.

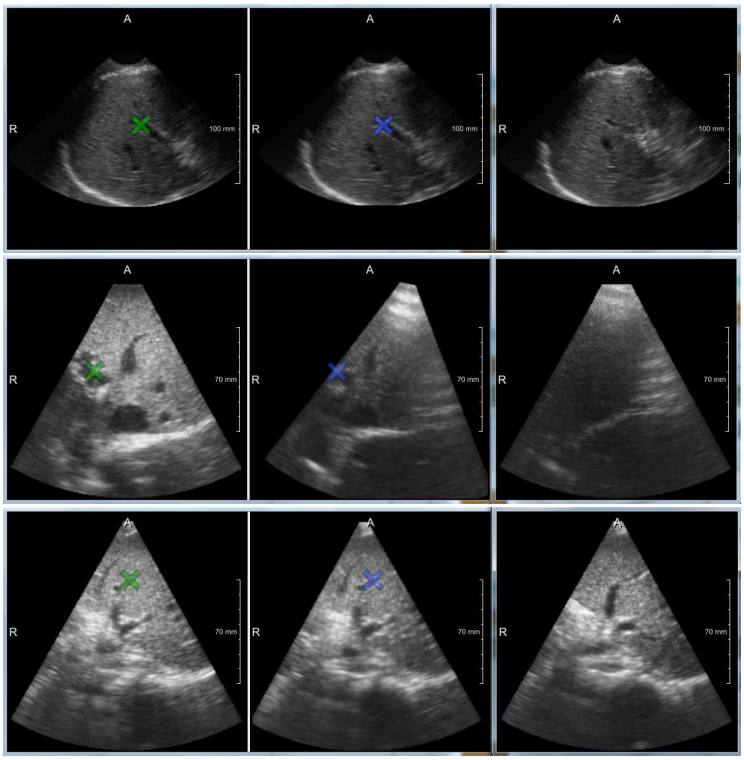

Fig. 5. Test set registered Volumes: Left - Reference image manual annotation, Middle - Registration result automatic annotation, Right - Moving Image. Row 1 - dataset EMC-04_1, time point 124; Row 2 - dataset SMT-05_1, time point 66; Row 3 - dataset SMT-07_2, time point 74.

The mean tracking error for the training set is 3.26 ± 2.62 mm. Two of the datasets (EMC-03_1, SMT-04_1) from the training set have large tracking errors, see Figure 3. In the EMC-03_1 4D US sequence the anatomical landmark is located on a vessel which undergoes large deformations due to blood flow and in the SMT-04_1 4D US sequence the anatomical landmark is located outside the liver. Some of the tracking results from the training set are shown in Figure 4. In the test set the SMT-05_1 4D sequence has large tracking error. In rest of the dataset the tracking performance is satisfactory. Some representative test set registration results are shown in Figure 5.

The speed depends on the number of points, search range size, number of samples in the search range (step size), block size and number of samples in the block. The current approach runs at 11 seconds per frame. For tracking of liver, real-time (faster than image temporal resolution) speed is achieved by Banerjee et al. [2] by selecting appropriate parameters for the US data acquired from Philips iU22 machine with X6-1 probe.

To conclude, we extended our current registration approaches for 3D and 4D US volumes such that it enables tracking of anatomical landmarks in 4D US

sequences. The method is evaluated using CLUST 2015 challenge datasets. For a test set of eight 4D US sequences, an accuracy of 1.62 ± 0.94 mm is achieved.

References

1. Arun, K.S., Huang, T.S., Blostein, S.D.: Least-squares fitting of two 3-D point sets. IEEE Trans. Pattern Anal. Mach. Intell. 9(5), 698–700 (1987)
2. Banerjee, J., Klink, C., Niessen, W.J., Moelker, A., van Walsum, T.: 4D ultrasound tracking of liver and its verification for TIPS guidance. IEEE Transactions on Medical Imaging (In press)
3. Banerjee, J., Klink, C., Peters, E.D., Niessen, W.J., Moelker, A., van Walsum, T.: Fast and robust 3D ultrasound registration - block and game theoretic matching. Medical Image Analysis 20(1), 173–183 (2015), http://dx.doi.org/10.1016/j.media.2014.11.004
4. Bell, M.A.L., Byram, B.C., Harris, E.J., Evans, P.M., Bamber, J.C.: In vivo liver tracking with a high volume rate 4D ultrasound scanner and a 2D matrix array probe. Physics in Medicine and Biology 57(5), 1359 (2012), http://stacks.iop.org/0031-9155/57/i=5/a=1359
5. Cifor, A., Risser, L., Chung, D., Anderson, E., Schnabel, J.: Hybrid feature-based diffeomorphic registration for tumor tracking in 2-D liver ultrasound images. Medical Imaging, IEEE Transactions on 32(9), 1647–1656 (2013)
6. Lediju, M., Byram, B., Harris, E., Evans, P., Bamber, J.: 3D liver tracking using a matrix array: Implications for ultrasonic guidance of IMRT. In: Ultrasonics Symposium (IUS), 2010 IEEE. pp. 1628–1631 (Oct 2010)
7. Luca, V.D., Benz, T., Kondo, S., König, L., Lübke, D., Rothlübbers, S., Somphone, O., Allaire, S., Bell, M.A.L., Chung, D.Y.F., Cifor, A., Grozea, C., Günther, M., Jenne, J., Kipshagen, T., Kowarschik, M., Navab, N., Rühaak, J., Schwaab, J., Tanner, C.: The 2014 liver ultrasound tracking benchmark. Physics in Medicine and Biology 60(14), 5571 (2015), http://stacks.iop.org/0031-9155/60/i=14/a=5571
8. De Luca, V., Tschannen, M., Székely, G., Tanner, C.: A learning-based approach for fast and robust vessel tracking in long ultrasound sequences. In: MICCAI (1). pp. 518–525 (2013)
9. Øye, O.K., Wein, W., Ulvang, D.M., Matre, K., Viola, I.: Real time image-based tracking of 4D ultrasound data. In: MICCAI (1). pp. 447–454 (2012)
10. Preiswerk, F., Luca, V.D., Arnold, P., Celicanin, Z., Petrusca, L., Tanner, C., Bieri, O., Salomir, R., Cattin, P.C.: Model-guided respiratory organ motion prediction of the liver from 2D ultrasound. Medical Image Analysis 18(5), 740–751 (2014), http://dx.doi.org/10.1016/j.media.2014.03.006
11. Schneider, R.J., Perrin, D.P., Vasilyev, N.V., Marx, G.R., del Nido, P.J., Howe, R.D.: Real-time image-based rigid registration of three-dimensional ultrasound. Medical Image Analysis 16(2), 402–414 (2012)
12. Vijayan, S., Klein, S., Hofstad, E.F., Lindseth, F., Ystgaard, B., Langø, T.: Motion tracking in the liver: Validation of a method based on 4D ultrasound using a nonrigid registration technique. Medical Physics 41(8), 082903 (2014), http://scitation.aip.org/content/aapm/journal/medphys/41/8/10.1118/1.4890091